Acta Mechanica Sinica (2013) 29(6):763–772
DOI 10.1007/s10409-013-0088-0

RESEARCH PAPER

Inspection of free energy functions in gradient crystal plasticity

Samuel Forest · Nicolas Guéninchault

Received: 8 July 2013 / Revised: 26 August 2013 / Accepted: 29 October 2013

Abstract The dislocation density tensor computed as the curl of plastic distortion is regarded as a new constitutive variable in crystal plasticity. The dependence of the free energy function on the dislocation density tensor is explored starting from a quadratic ansatz. Rank one and logarithmic dependencies are then envisaged based on considerations from the statistical theory of dislocations. The relevance of the presented free energy potentials is evaluated from the corresponding analytical solutions of the periodic two-phase laminate problem under shear where one layer is a single crystal material undergoing single slip and the second one remains purely elastic.

Keywords Gradient plasticity · Crystal plasticity · Continuum thermodynamics · Dislocation density tensor · Read–Shockley energy

1 Introduction

The dislocation density tensor, as initially defined in Refs. [1, 2] and recently revisited in Refs. [3, 4], is now recognized as a true constitutive variable to be introduced in the crystal plasticity theory. Single crystal materials and grains in polycrystal can store energy by increasing the densities of so-called geometrically necessary dislocations directly related to the dislocation density tensor. The partial derivative of the free energy density function delivers a generalized stress having the physical dimension of couple stresses. Accordingly, the crystal plasticity theory must be extended to the mechanics of generalized continua that includes strain gradient plasticity and micromorphic models [5]. Linearized theories for crystals containing dislocations and disclinations have been recently presented in Ref. [6]. The non-linear elastic-plastic regime is the realm of strain gradient crystal plasticity theory as explored in Refs. [7–10].

S. Forest (✉) · N. Guéninchault
Centre des Matériaux, Mines ParisTech, CNRS UMR 7633
BP 87, 91003 Evry Cedex, France
e-mail: samuel.forest@ensmp.fr

We concentrate on theories introducing the full dislocation density tensor and not the individual contributions of each slip system. The reason is the computational inefficiency of the latter model class which requires to introduce, at least, as many additional degrees of freedom as slip systems. In contrast, finite element simulations based on models including the full dislocation tensor always require the same number of additional degrees of freedom, irrespective of the number of slip systems which can strongly differ for FCC, BCC and HCP metals and alloys for instance.

Little is known about the relevant form of the free energy density function. A quadratic free energy potential was first proposed in Ref. [11] and further investigated in Refs. [9, 12, 13]. It leads to a linear relationship between the generalized stress tensor and the dislocation density tensor. Computational analyses based on such a quadratic ansatz were then performed by Refs. [14–19]. In contrast a homogeneous function of degree one of the norm of the dislocation density tensor was proposed in Refs. [20, 21]. Inspiration can also be found in the free energy functionals proposed in the class of strain gradient plasticity models that are based on the individual densities of geometrically necessary dislocations (GND) attached to each slip system. The effective free energy in Ref. [22] contains a contribution in $\rho \log \rho$ where ρ is the total dislocation density, and a quadratic term in the GND content. The internal energy density in Ref. [23] includes a single logarithmic term in the total dislocation density. As for them, Svendsen and Bargmann [24] introduce free energy densities depending on the absolute slip system related GND densities and also on the product of density and its logarithm, thus following Groma. They also split the function into contributions of screw and edge dislocation parts.

The objective of the present paper is to investigate the relevance of various forms of the free energy density functions including new ones motivated from dislocation theory, by solving a boundary value problem on a laminate microstructure. The predicted plastic slip distribution and the corresponding size effects will be discussed to assess the physical relevance of the proposed models. For instance, a

$1/\ell$ size-dependence of the stress at given plastic strain as a function of the thickness ℓ of the laminate unit cell was predicted by Ref. [25] whereas a $1/\ell^2$ dependence was found by Ref. [10].

The kinematics and balance equations of the strain gradient plasticity theory are recalled in Sect. 2. The laminate boundary value problem is defined in Sect. 3. The corresponding solutions for the quadratic and rank one models are given in Subsects. 3.1 and 3.2, respectively. New energy potentials are proposed and discussed in Sects. 4 and 5.

First, second and fourth order tensors are respectively denoted by $\underline{\boldsymbol{a}}$, $\underline{\underline{\boldsymbol{a}}}$, and $\underline{\underline{\underline{\underline{\boldsymbol{a}}}}}$. The theory is formulated within the small perturbation framework. Vector $\underline{\boldsymbol{x}}$ denotes the position of the material point. The scalar, vector and tensor products are written "$\cdot$", "$\times$", "$\otimes$", respectively. The differential operators are defined in the following way with respect to a Cartesian coordinate basis $(\underline{\boldsymbol{e}}_i)_{i=1,3}$

$$\operatorname{grad} \underline{\boldsymbol{a}} = \frac{\partial \underline{\boldsymbol{a}}}{\partial x_j} \otimes \underline{\boldsymbol{e}}_j = a_{i,j} \underline{\boldsymbol{e}}_i \otimes \underline{\boldsymbol{e}}_j, \tag{1}$$

$$\operatorname{div} \underline{\underline{\boldsymbol{a}}} = \frac{\partial \underline{\underline{\boldsymbol{a}}}}{\partial x_j} \cdot \underline{\boldsymbol{e}}_j = a_{ij,j} \underline{\boldsymbol{e}}_i, \tag{2}$$

$$\operatorname{curl} \underline{\underline{\boldsymbol{a}}} = \frac{\partial \underline{\underline{\boldsymbol{a}}}}{\partial x_k} \times \underline{\boldsymbol{e}}_k = \epsilon_{jkl} a_{ij,k} \underline{\boldsymbol{e}}_i \otimes \underline{\boldsymbol{e}}_l. \tag{3}$$

Use is also made of the permutation third order tensor $\underline{\underline{\underline{\boldsymbol{\epsilon}}}}$.

2 Formulation of the curl $\boldsymbol{H}^{\mathrm{p}}$ model

The motion of the material points of the continuum is described by the displacement vector field $\underline{\boldsymbol{u}}(\underline{\boldsymbol{x}})$. The gradient of the displacement is called $\underline{\underline{\boldsymbol{H}}}$. It is split into its elastic and plastic contributions

$$\underline{\underline{\boldsymbol{H}}} = \operatorname{grad} \underline{\boldsymbol{u}} = \underline{\underline{\boldsymbol{H}}}^{\mathrm{e}} + \underline{\underline{\boldsymbol{H}}}^{\mathrm{p}}, \tag{4}$$

where $\underline{\underline{\boldsymbol{H}}}^{\mathrm{e}}$ and $\underline{\underline{\boldsymbol{H}}}^{\mathrm{p}}$ called the elastic and plastic deformations, respectively. The displacement gradient, and its elastic and plastic parts are decomposed into their symmetric parts, the strains, and their skew-symmetric parts, the infinitesimal rotations

$$\underline{\underline{\boldsymbol{H}}} = \underline{\underline{\boldsymbol{\varepsilon}}} + \underline{\underline{\boldsymbol{\omega}}}, \tag{5}$$

$$\underline{\underline{\boldsymbol{H}}}^{\mathrm{e}} = \underline{\underline{\boldsymbol{\varepsilon}}}^{\mathrm{e}} + \underline{\underline{\boldsymbol{\omega}}}^{\mathrm{e}}, \tag{6}$$

$$\underline{\underline{\boldsymbol{H}}}^{\mathrm{p}} = \underline{\underline{\boldsymbol{\varepsilon}}}^{\mathrm{p}} + \underline{\underline{\boldsymbol{\omega}}}^{\mathrm{p}}. \tag{7}$$

The dislocation density tensor is defined as

$$\underline{\underline{\boldsymbol{\Gamma}}} = \operatorname{curl} \underline{\underline{\boldsymbol{H}}}^{\mathrm{p}} = -\operatorname{curl} \underline{\underline{\boldsymbol{H}}}^{\mathrm{e}}, \tag{8}$$

following Refs. [3, 4, 26]. Since elastic and plastic deformations are generally not compatible fields, in contrast to $\underline{\underline{\boldsymbol{H}}}$, the dislocation density tensor generally does not vanish.

Introducing such a new quantity in the continuum model requires an extension of the classical Cauchy continuum because the model involves not only the gradient of the displacement field but also some combinations of the components of the gradient of the plastic deformation field $\underline{\underline{\boldsymbol{H}}}^{\mathrm{p}}$. The classical power of internal forces is enhanced by powers involving generalized stresses that are conjugate to the plastic deformation rate and dislocation density tensor rate

$$p^{(i)} = \underline{\underline{\boldsymbol{\sigma}}} : \dot{\underline{\underline{\boldsymbol{\varepsilon}}}} + \underline{\underline{\boldsymbol{s}}} : \dot{\underline{\underline{\boldsymbol{H}}}}^{\mathrm{p}} + \underline{\underline{\underline{\boldsymbol{M}}}} : \operatorname{curl} \dot{\underline{\underline{\boldsymbol{H}}}}^{\mathrm{p}}, \tag{9}$$

where $\underline{\underline{\boldsymbol{\sigma}}}$, only, is a symmetric second order stress tensor. The generally non symmetric stress tensor $\underline{\underline{\boldsymbol{s}}}$ is conjugate to the plastic deformation rate. The physical dimension of $\underline{\underline{\underline{\boldsymbol{M}}}}$ justifies the name of double-stress tensor.

The Cauchy simple-stress tensor $\underline{\underline{\boldsymbol{\sigma}}}$ fulfills the standard balance and boundary conditions on the material body Ω with boundary $\partial\Omega$

$$\operatorname{div} \underline{\underline{\boldsymbol{\sigma}}} = 0, \quad \forall \underline{\boldsymbol{x}} \in \Omega, \tag{10}$$

in the absence of volume nor inertial forces

$$\underline{\boldsymbol{t}} = \underline{\underline{\boldsymbol{\sigma}}} \cdot \underline{\boldsymbol{n}}, \quad \forall \underline{\boldsymbol{x}} \in \partial\Omega, \tag{11}$$

where $\underline{\boldsymbol{t}}$ is the usual traction vector. The generalized stresses fulfill additional balance and boundary conditions

$$\operatorname{curl} \underline{\underline{\underline{\boldsymbol{M}}}} + \underline{\underline{\boldsymbol{s}}} = \boldsymbol{0}, \quad \forall \underline{\boldsymbol{x}} \in \Omega, \tag{12}$$

$$\underline{\underline{\boldsymbol{m}}} = \underline{\underline{\underline{\boldsymbol{M}}}} \cdot \underline{\underline{\underline{\boldsymbol{\epsilon}}}} \cdot \underline{\boldsymbol{n}}, \quad \forall \underline{\boldsymbol{x}} \in \partial\Omega, \tag{13}$$

where $\underline{\underline{\boldsymbol{m}}}$ is called the double traction and corresponds to a surface density of double forces.

This continuum theory is called the "curl $\boldsymbol{H}^{\mathrm{p}}$" model in Ref. [10] where the previous field and boundary conditions are derived.

The usual state variables of isothermal plasticity theory are the elastic strain and some internal variables including for instance the scalar dislocation density ρ^s for each slip system s, known as the length of dislocation lines per unit volume. As advocated by Kröner [27], the scalar and tensor dislocation densities are independent statistical measures of the dislocation population in the material volume element. They should be both introduced in the set of state variables. That is why it is proposed to introduce the dislocation density tensor in the arguments of the free energy volume density function

$$\psi(\underline{\underline{\boldsymbol{\varepsilon}}}^{\mathrm{e}}, \rho^s, \underline{\underline{\boldsymbol{\Gamma}}})$$

as originally proposed in Ref. [11]. The dissipation inequality is written as

$$p^{(i)} - \dot{\psi} \geqslant 0. \tag{14}$$

The following state laws are adopted

$$\underline{\underline{\boldsymbol{\sigma}}} = \frac{\partial \psi}{\partial \underline{\underline{\boldsymbol{\varepsilon}}}^{\mathrm{e}}}, \tag{15}$$

$$R^s = \frac{\partial \psi}{\partial \rho^s}, \tag{16}$$

$$\underline{\underline{\underline{\boldsymbol{M}}}} = \frac{\partial \psi}{\partial \underline{\underline{\boldsymbol{\Gamma}}}}, \tag{17}$$

where R^s is the thermodynamic force associated with the internal variable ρ^s [28]. As a result, the dissipation rate is reduced to

$$(\underset{\sim}{\boldsymbol{\sigma}} + \underset{\sim}{\boldsymbol{s}}) : \dot{\underset{\sim}{\boldsymbol{H}}}^{\mathrm{p}} - \sum_s R^s \dot{\rho}^s \geqslant 0. \tag{18}$$

In crystal plasticity, plastic flow is due to slip processes according to slip systems

$$\dot{\underset{\sim}{\boldsymbol{H}}}^{\mathrm{p}} = \sum_s \dot{\gamma}^s \underline{\boldsymbol{\ell}}^s \otimes \underline{\boldsymbol{n}}^s, \tag{19}$$

where each slip system s is characterized by the slip direction $\underline{\boldsymbol{\ell}}^s$ and the normal vector to the slip plane $\underline{\boldsymbol{n}}^s$, γ^s being the corresponding amount of slip. The dissipation rate (19) then takes the form

$$\sum_s (\tau^s - x^s)\dot{\gamma}^s - \sum_s R^s \dot{\rho}^s \geqslant 0, \tag{20}$$

with the resolved shear stress

$$\tau^s = \underset{\sim}{\boldsymbol{\sigma}} : \underline{\boldsymbol{\ell}}^s \otimes \underline{\boldsymbol{n}}^s \tag{21}$$

and the back stress

$$x^s = -\underset{\sim}{\boldsymbol{s}} : \underline{\boldsymbol{\ell}}^s \otimes \underline{\boldsymbol{n}}^s = \operatorname{curl} \underset{\sim}{\boldsymbol{M}} : \underline{\boldsymbol{\ell}}^s \otimes \underline{\boldsymbol{n}}^s. \tag{22}$$

This prompts us to postulate a generalized Schmid law stipulating that plastic slip will occur on slip system s as soon as a critical resolved shear stress value τ_{c}^s is reached

$$|\tau^s - x^s| = \tau_{\mathrm{c}}^s. \tag{23}$$

3 Shearing of an elastic-plastic two-phase laminate

Laminate microstructures are prone to size effects especially in the case of metals for which the interfaces act as barriers against dislocations. The material response then strongly depends on the layer thickness. This situation has been considered for Cosserat, micromorphic and strain gradient single crystals under single and double slip in Refs. [10, 12, 15, 29]. The laminate is a periodic arrangement of two phases including a purely elastic material and a plastic strain gradient layer. The unit cell corresponding to this arrangement is shown in Fig. 1. It is periodic along all three directions of the space. It must be replicated in the three directions so as to obtain the complete multilayer material. The thickness of the hard elastic layer is h, whereas the thickness of the soft plastic layer, endowed with the "curl $\boldsymbol{H}^{\mathrm{p}}$" material behaviour, is s. The unit cell size is $l = s + h$ and the soft phase volume fraction is $f = s/l$. Both phases are assumed to share the same elastic properties for simplicity. More general results, but without fundamental difference, may be derived from Ref. [10].

The unit cell of Fig. 1 is subjected to a mean simple shear $\bar{\gamma}$ in direction 1. The origin O of the coordinate system is the center of the soft phase. The displacement field is of the form

$$u_1 = \bar{\gamma} x_2, \quad u_2(x_1) = u(x_1), \quad u_3 = 0, \tag{24}$$

where $u(x_1)$ is a periodic function which describes the deviation from the homogeneous shear. This fluctuation is the main unknown of the boundary value problem. The gradient of the displacement field and strain tensors are computed as follows

$$\nabla \underline{\boldsymbol{u}} = \begin{bmatrix} 0 & \bar{\gamma} & 0 \\ u_{,1} & 0 & 0 \\ 0 & 0 & 0 \end{bmatrix},$$
$$\underset{\sim}{\boldsymbol{\varepsilon}} = \begin{bmatrix} 0 & \frac{1}{2}(\bar{\gamma} + u_{,1}) & 0 \\ \frac{1}{2}(\bar{\gamma} + u_{,1}) & 0 & 0 \\ 0 & 0 & 0 \end{bmatrix}, \tag{25}$$

where $u_{,1}$ denotes the first derivative of the displacement u with respect to x_1.

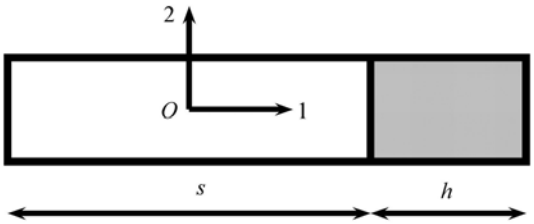

Fig. 1 Unit cell of the two-phase laminate made of an elastic-plastic phase s and an elastic phase h

One single slip system is assumed to be activated in the soft phase with the slip direction $\underline{\boldsymbol{\ell}} = \underline{\boldsymbol{e}}_1$ and the normal to the slip plane $\underline{\boldsymbol{n}} = \underline{\boldsymbol{e}}_2$. This situation will lead to a piling-up of dislocations with opposite signs at the interfaces $x_1 = \pm s/2$. According to Eq. (19), the plastic deformation takes then the form

$$\underset{\sim}{\boldsymbol{H}}^{\mathrm{p}} = \begin{bmatrix} 0 & \gamma & 0 \\ 0 & 0 & 0 \\ 0 & 0 & 0 \end{bmatrix}, \tag{26}$$

where $\gamma(x_1)$ is the second main unknown field of the problem. After Hooke's law, the only activated simple stress component is σ_{12}. Due to the balance of momentum equation and the continuity of the traction vector, this stress component is homogeneous throughout the laminate. The simple stress tensor is computed according to Hooke's law for linear isotropic elasticity

$$\underset{\sim}{\boldsymbol{\sigma}} = \mu \begin{bmatrix} 0 & \bar{\gamma} + u_{,1} - \gamma & 0 \\ \bar{\gamma} + u_{,1} - \gamma & 0 & 0 \\ 0 & 0 & 0 \end{bmatrix}. \tag{27}$$

The dislocation density tensor (8) is then computed as

$$\underset{\sim}{\boldsymbol{\Gamma}} = \operatorname{curl} \underset{\sim}{\boldsymbol{H}}^{\mathrm{p}} = \begin{bmatrix} 0 & 0 & -\gamma_{,1} \\ 0 & 0 & 0 \\ 0 & 0 & 0 \end{bmatrix}. \tag{28}$$

The elasticity law in the elastic phase and the elastic-plastic response of the soft phase are then exploited in the next sec-

tions based on specific choices for the free energy potential to derive the partial differential equations for plastic strain and, finally, for the displacement fluctuation. The explicit solution is found after considering precise interface conditions regarding continuity of various variables at interfaces.

3.1 Size effect for a quadratic potential

Linear constitutive equations are first considered, associated with a quadratic potential in the form

$$\Psi(\underset{\sim}{\boldsymbol{\varepsilon}}^{\mathrm{e}}, \operatorname{curl} \underset{\sim}{\boldsymbol{H}}^{\mathrm{p}}) = \frac{1}{2}\underset{\sim}{\boldsymbol{\varepsilon}}^{\mathrm{e}} : \underset{\approx}{\boldsymbol{C}} : \underset{\sim}{\boldsymbol{\varepsilon}}^{\mathrm{e}} + \frac{1}{2}\operatorname{curl} \underset{\sim}{\boldsymbol{H}}^{\mathrm{p}} : \underset{\approx}{\boldsymbol{A}} : \operatorname{curl} \underset{\sim}{\boldsymbol{H}}^{\mathrm{p}}, \quad (29)$$

where $\underset{\approx}{\boldsymbol{C}}$ denotes the usual tensor of elastic moduli and $\underset{\approx}{\boldsymbol{A}}$ is a new fourth order tensor of generalised moduli. For the sake of simplicity no internal variable is considered in the analysis. This leads to the following linear state laws

$$\underset{\sim}{\boldsymbol{\sigma}} = \underset{\approx}{\boldsymbol{C}} : \underset{\sim}{\boldsymbol{\varepsilon}}^{\mathrm{e}}, \quad \underset{\sim}{\boldsymbol{M}} = \underset{\approx}{\boldsymbol{A}} : \operatorname{curl} \underset{\sim}{\boldsymbol{H}}^{\mathrm{p}}. \quad (30)$$

In the isotropic case, the linear constitutive relation between the dislocation density tensor and the double stress tensor is characterized by three independent moduli, due to the fact that $\underset{\sim}{\boldsymbol{\Gamma}}$ is generally not symmetric. In the following analytical derivation, a simplified constitutive law is adopted in the spirit of Ref. [30] that involves a single new modulus A (unit MPa·mm^2)

$$\underset{\sim}{\boldsymbol{M}} = A \operatorname{curl} \underset{\sim}{\boldsymbol{H}}^{\mathrm{p}}. \quad (31)$$

This corresponds to a potential of the form

$$\Psi(\underset{\sim}{\boldsymbol{\varepsilon}}^{\mathrm{e}}, \operatorname{curl} \underset{\sim}{\boldsymbol{H}}^{\mathrm{p}}) = \frac{1}{2}\underset{\sim}{\boldsymbol{\varepsilon}}^{\mathrm{e}} : \underset{\approx}{\boldsymbol{C}} : \underset{\sim}{\boldsymbol{\varepsilon}}^{\mathrm{e}} + \frac{1}{2}A\|\operatorname{curl} \underset{\sim}{\boldsymbol{H}}^{\mathrm{p}}\|^2. \quad (32)$$

This simplifying assumption was first made in Ref. [11]. The expression of the back stress can now be worked out from Eq. (22)

$$x^s = (\operatorname{curl} \underset{\sim}{\boldsymbol{M}}) : \underline{\boldsymbol{\ell}}^s \otimes \underline{\boldsymbol{n}}^s = A(\operatorname{curl} \underset{\sim}{\boldsymbol{H}}^{\mathrm{p}}) : \underline{\boldsymbol{\ell}}^s \otimes \underline{\boldsymbol{n}}^s, \quad (33)$$

assuming piece-wise constant distribution of A parameter. It is remarkable that the expression involves second derivatives of plastic deformation. This dependence on the second derivative of slip is reminiscent of Aifantis strain gradient plasticity model [31, 32]. However, a significant difference in the present model is that the obtained strain gradient hardening is of kinematic nature whereas Aifantis considered isotropic hardening.

In the case of the two-phase laminate problem, the double stress tensor takes the form

$$\underset{\sim}{\boldsymbol{M}} = A \begin{bmatrix} 0 & 0 & -\gamma_{,1} \\ 0 & 0 & 0 \\ 0 & 0 & 0 \end{bmatrix}. \quad (34)$$

The curl of the double stress tensor is then computed as

$$\operatorname{curl} \underset{\sim}{\boldsymbol{M}} = A \begin{bmatrix} 0 & -\gamma_{,11} & 0 \\ 0 & 0 & 0 \\ 0 & 0 & 0 \end{bmatrix} \quad (35)$$

from which the back stress is found to be proportional to the second derivative of slip in the direction of slip

$$x = -A\gamma_{,11}. \quad (36)$$

The application of the generalized Schmid law for slip in direction 1 gives

$$\tau = \sigma_{12} = \tau_{\mathrm{c}} + x = \tau_{\mathrm{c}} - A\gamma_{,11}. \quad (37)$$

The shear stress component σ_{12} being uniform in the laminate, it follows from the previous equation that plastic slip γ has a parabolic profile. The interface condition of vanishing slip $\gamma\left(\pm\frac{s}{2}\right) = 0$, due to the fact that dislocations cannot cross nor accumulate in the interface, is used to determine some of the integration constants and find

$$\gamma(x_1) = \alpha\left(x_1^2 - \frac{s^2}{4}\right). \quad (38)$$

The shear stress is related to the displacement in the elastic phase $u(x_1) = u^h(x_1)$ and $u(x_1) = u^s(x_1)$ in the soft phase by

$$\sigma_{12} = \mu(u^h_{,1} + \bar{\gamma}), \quad \sigma_{12} = \mu(u^s_{,1} + \bar{\gamma} - \gamma), \quad (39)$$

which implies that

$$u^h(x_1) = Cx_1 + D, \quad u^s(x_1) = \alpha\frac{x_1^3}{3} + \left(C - \alpha\frac{s^2}{4}\right)x_1, \quad (40)$$

where the integration constants α, C, D remain to be determined by means of three additional interface conditions.

The continuity of the displacement at $x_1 = s/2$ requires

$$u^s\left(\frac{s}{2}\right) = u^h\left(\frac{s}{2}\right) \Longrightarrow D = -\frac{s^3\alpha}{12}. \quad (41)$$

Periodicity of displacement entails

$$u^s\left(-\frac{s}{2}\right) = u^h\left(-\frac{s}{2} + \ell\right) \Longrightarrow C\ell + D = \frac{s^3\alpha}{12}. \quad (42)$$

Continuity of the shear stress at $x_1 = s/2$ gives

$$\tau_{\mathrm{c}} - 2A\alpha = \mu(C + \bar{\gamma}) \quad (43)$$

and finally

$$C = \frac{\tau_{\mathrm{c}} - \mu\bar{\gamma}}{\mu + \dfrac{12A\ell}{s^3}}. \quad (44)$$

The obtained profiles of slip and displacement are given in Fig. 2 for the material parameters of Table 1 chosen for the illustration.

At the end, the overall stress is expressed as a function of overall shear

$$\sigma_{12} = \tau_{\mathrm{c}} + \frac{\mu}{1 + \dfrac{\mu s^3}{12A\ell}}\left(\bar{\gamma} - \frac{\tau_{\mathrm{c}}}{\mu}\right). \quad (45)$$

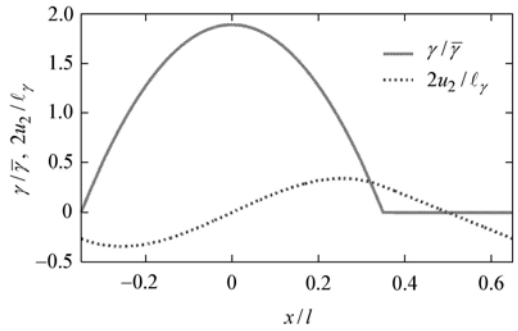

Fig. 2 Profiles of the normalized slip and displacement in the laminate (quadratic potential, $\bar{\gamma} = 0.01$, $\sigma_{12} = 36\,\text{MPa}$)

Table 1 Material and geometric parameters of a laminate microstructure made of strain gradient crystal plasticity material endowed with a quadratic free energy density

μ/MPa	τ_c/MPa	A/(MPa·mm^2)	f	ℓ/μm	$\bar{\gamma}$
30 000	20	0.005	0.7	10	0.01

The stress can also be expressed as a function of the mean slip

$$\begin{aligned}\langle\gamma\rangle &= \frac{1}{\ell}\int_{-s/2}^{s/2}\gamma(x_1)\mathrm{d}x_1\\ &= f\Big(\bar{\gamma}-\frac{\sigma_{12}}{\mu}\Big)+\frac{1}{\ell}\Big(u^s\Big(\frac{s}{2}\Big)-u^s\Big(-\frac{s}{2}\Big)\Big)\\ &= f\Big(\bar{\gamma}-\frac{\sigma_{12}}{\mu}\Big)-C(1-f).\end{aligned}\tag{46}$$

The combination of Eqs. (45) and (46) leads to the following linear hardening rule

$$\sigma_{12} = \tau_c + \frac{12A}{f^3\ell^2}\langle\gamma\rangle.\tag{47}$$

This expression clearly shows the existence of the pile-up induced work-hardening. The hardening modulus is found to be proportional to the new parameter A and to be inversely proportional to the square of the unit cell size. In the limit of thick layers the constant stress τ_c is retrieved whereas hardening becomes infinite for smaller and smaller sizes. The obtained linear kinematic hardening is illustrated in Fig. 3 for the set of parameters of Table 1.

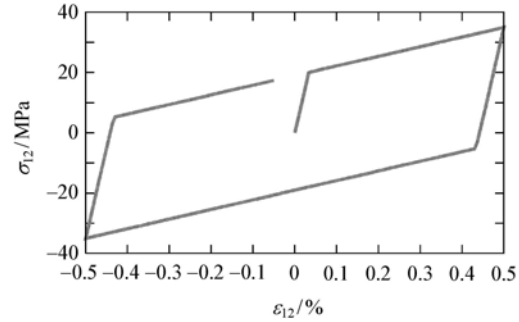

Fig. 3 Hysteresis loop for cyclic periodic shear test of the laminated $\bar{\gamma} = \pm 0.01$

The size dependence in $1/\ell^2$ is quite unusual in physical metallurgy so that the model should be modified in order to reach more realistic scaling laws [33]. It is proposed to modify the dependence of the free energy density on the dislocation density tensor.

3.2 Solution for a rank one potential

The norm of the dislocation density tensor is a measure of the density of geometrically dislocations ρ_G according to the terminology introduced by Ashby [34]

$$\Gamma = \|\mathrm{curl}\,\underset{\sim}{\boldsymbol{H}}^p\| = \sqrt{\mathrm{curl}\,\underset{\sim}{\boldsymbol{H}}^p : \mathrm{curl}\,\underset{\sim}{\boldsymbol{H}}^p} \sim \rho_G b,\tag{48}$$

where b is the norm of the Burgers vector.

A direct dependence of the free energy density on the norm of the dislocation density tensor has been proposed by several authors instead of the previous quadratic potential [20, 35, 36]

$$\psi(\underset{\sim}{\boldsymbol{\varepsilon}}^e, \mathrm{curl}\,\underset{\sim}{\boldsymbol{H}}^p) = \frac{1}{2}\underset{\sim}{\boldsymbol{\varepsilon}}^e : \underset{\approx}{\boldsymbol{C}} : \underset{\sim}{\boldsymbol{\varepsilon}}^e + A\|\mathrm{curl}\,\underset{\sim}{\boldsymbol{H}}^p\|.\tag{49}$$

Note that the contribution in $\Gamma = \|\mathrm{curl}\,\underset{\sim}{\boldsymbol{H}}^p\|$ is not differentiable at $\underset{\sim}{\boldsymbol{\Gamma}} = \boldsymbol{0}$. The new state law for the double stress tensor then is

$$\underset{\sim}{\boldsymbol{M}} = A\frac{\mathrm{curl}\,\underset{\sim}{\boldsymbol{H}}^p}{\|\mathrm{curl}\,\underset{\sim}{\boldsymbol{H}}^p\|} = A\frac{\underset{\sim}{\boldsymbol{\Gamma}}}{\Gamma}.\tag{50}$$

In the case of the two-phase laminate

$$\underset{\sim}{\boldsymbol{\Gamma}} = -\gamma_{,1}\underline{\boldsymbol{e}}_1\otimes\underline{\boldsymbol{e}}_3 \Longrightarrow \underset{\sim}{\boldsymbol{M}} = -A\,\mathrm{sign}\gamma_{,1}\underline{\boldsymbol{e}}_1\otimes\underline{\boldsymbol{e}}_3.\tag{51}$$

The double stress tensor is therefore piece-wise constant in the soft phase. It follows that the back stress x given by Eq. (23) vanishes almost everywhere. The size effect induced by the discontinuity of plastic strain at the interface, associated with a dislocation wall, will be studied in the forthcoming work [37]. The authors in Ref. [35] have found a size effect for a spherical grain subjected to Dirichlet boundary conditions, based on the same potential. For this grain geometry, the higher order stress is not piece-wise constant and is related to the curvature of the surface.

4 Logarithmic free energy potential

As a next candidate for the formulation of the free energy density dependence on the dislocation density tensor, the following expression is proposed

$$\psi(\underset{\sim}{\boldsymbol{\varepsilon}}^e, \underset{\sim}{\boldsymbol{\Gamma}}) = \frac{1}{2}\underset{\sim}{\boldsymbol{\varepsilon}}^e : \underset{\approx}{\boldsymbol{C}} : \underset{\sim}{\boldsymbol{\varepsilon}}^e + A\frac{\|\underset{\sim}{\boldsymbol{\Gamma}}\|}{\Gamma_0}\Big(\log\frac{\|\underset{\sim}{\boldsymbol{\Gamma}}\|}{\Gamma_0}-1\Big),\tag{52}$$

where A and Γ_0 are material parameters. This choice is motivated from a statistical dislocation theory presented in Subsect. 4.1. Parameter Γ_0 is regarded as the initial value of the norm of the dislocation density tensor $\Gamma = \|\underset{\sim}{\boldsymbol{\Gamma}}\|$. The energy density function (52) then is an increasing convex function of $\Gamma \geqslant \Gamma_0$.

The state laws of the model are

$$\underset{\sim}{\boldsymbol{\sigma}} = \underset{\approx}{\boldsymbol{C}} : \underset{\sim}{\boldsymbol{\varepsilon}}^{\mathrm{e}}, \quad \underset{\sim}{\boldsymbol{M}} = \frac{A}{\Gamma_0} \log\left(\frac{\Gamma}{\Gamma_0}\right) \frac{\underset{\sim}{\boldsymbol{\Gamma}}}{\Gamma}. \tag{53}$$

4.1 Motivation from the statistical theory of dislocations

The existence of a back stress induced by dislocations structures also arises in the statistical theory of dislocations as developed by Groma for single slip of edge dislocations [38]. It can be estimated in terms of the gradient of density of geometrically necessary dislocations as

$$x = \frac{\mu b \beta}{2\pi(1-\nu)\rho} \frac{\partial \rho_{\mathrm{G}}}{\partial x_1}, \tag{54}$$

where ρ is the total scalar dislocation density, β is a non-dimensional constant and direction 1 is the slip direction for the considered single slip system. It has been incorporated in the crystal plasticity theory in Ref. [39]. In the absence of statistically stored dislocations, $\rho = \rho_{\mathrm{G}}$ and the previous equation can be integrated as

$$x = \frac{\mu b \beta}{2\pi(1-\nu)} \frac{\partial}{\partial x_1} \log \rho_{\mathrm{G}}. \tag{55}$$

Keeping the expression (22) as a function of the double stress tensor, the previous relation is integrated twice in the form

$$M_{13} \sim \log \rho_{\mathrm{G}} \Longrightarrow \psi \sim \rho_{\mathrm{G}}(\log \rho_{\mathrm{G}} - 1). \tag{56}$$

Note however that this potential is not fully consistent with the statistical dislocation theory in Ref. [38] since it is based on the simplification $\rho \simeq \rho_{\mathrm{G}}$. A more realistic function will therefore include combined terms in the total dislocation density and in the GND content. The corresponding theory is left for future work since it may not be amenable to close form solutions of the differential equation to be solved in the next section.

4.2 Solution of the two-phase laminate problem

For the two-phase laminate, the double stress tensor according to Eq. (53) takes the value

$$\begin{aligned} \underset{\sim}{\boldsymbol{M}} &= -\frac{A}{\Gamma_0} \log\left(\frac{|\gamma_{,1}|}{\Gamma_0}\right) \frac{\gamma_{,1}}{|\gamma_{,1}|} \underline{\boldsymbol{e}}_1 \otimes \underline{\boldsymbol{e}}_3 \\ &= -\frac{A}{\Gamma_0} \epsilon \log \frac{|\gamma_{,1}|}{\Gamma_0} \underline{\boldsymbol{e}}_1 \otimes \underline{\boldsymbol{e}}_3, \end{aligned} \tag{57}$$

$$\mathrm{curl}\, \underset{\sim}{\boldsymbol{M}} = -\frac{A}{\Gamma_0} \frac{\gamma_{,11}}{|\gamma_{,1}|} \underline{\boldsymbol{e}}_1 \otimes \underline{\boldsymbol{e}}_2, \tag{58}$$

where $\epsilon = \mathrm{sign}\gamma_{,1}$. The induced back stress then is

$$x = \mathrm{curl}\, \underset{\sim}{\boldsymbol{M}} : \underline{\boldsymbol{e}}_1 \otimes \underline{\boldsymbol{e}}_2 = -\frac{A}{\Gamma_0} \frac{\gamma_{,11}}{|\gamma_{,1}|}. \tag{59}$$

The Schmid law requires that

$$\sigma_{12} = \tau = \tau_{\mathrm{c}} + x = \tau_{\mathrm{c}} - \frac{A}{\Gamma_0} \frac{\gamma_{,11}}{|\gamma_{,1}|}. \tag{60}$$

This is a differential equation in γ the solution of which is of the form

$$\gamma(x_1) = \alpha\left[\exp\left(\frac{s}{2L}\right) - \exp\left(-\epsilon \frac{x_1}{L}\right)\right], \tag{61}$$

where α is a constant to be determined and

$$\frac{1}{L} = \frac{\sigma_{12} - \tau_{\mathrm{c}}}{A} \Gamma_0. \tag{62}$$

The constant L has the physical dimension of length. It is positive for positive shear in direction 1 and under the assumption of plastic loading. The slip function (61) fulfills the conditions $\gamma\left(\pm \frac{s}{2}\right) = 0$. The shear stress can be used to compute the displacements in the soft and hard phases

$$\begin{aligned} u^s(x_1) = &\left[\frac{\sigma_{12}}{\mu} - \bar{\gamma} + \alpha \exp\left(\frac{s}{2L}\right)\right] x_1 \\ &+ \alpha L \epsilon \left[\exp\left(-\epsilon \frac{x_1}{L}\right) - 1\right], \end{aligned} \tag{63}$$

$$u^h(x_1) = \left(\frac{\sigma_{12}}{\mu} - \bar{\gamma}\right) x_1 + D. \tag{64}$$

The uniform translation in u^s was chosen such that it is continuous at $x_1 = 0$ and $u^s(0) = 0$.

The constants to be determined are α, D, and σ_{12} or, equivalently, L. Two conditions are obtained from the continuity requirement of the displacement at $s/2$ and at $s/2 + h$. From $u^s(s/2) = u^h(s/2)$, we get

$$D = \alpha\left[\left(\frac{s}{2} - L\right) \exp\left(\frac{s}{2L}\right) + L\right]. \tag{65}$$

From $u^s(-s/2) = u^h(s/2 + h)$, we get

$$D = \left(\bar{\gamma} - \frac{\sigma_{12}}{\mu}\right) \frac{\ell}{2}. \tag{66}$$

The two last relations have been obtained under the assumption that $\epsilon = -1$ for $x_1 \in [0 : s/2]$ and $\epsilon = 1$ for $x_1 \in [-s/2 : 0]$, which corresponds to an applied shear $\bar{\gamma} > 0$.

Detailed determination of coefficient α is given in Ref. [37] is given in Fig. 4 for given values of the shear stress and the values of material parameters coming from the Table 1, except that $A/\Gamma_0 = 0.03\,\mathrm{MPa{\cdot}mm}$. The profiles are exponential and differ from the parabolic one of Fig. 2. They are close to the cosh-solutions worked out in Ref. [29].

A regularization of the potential (52) can be proposed in the form

$$\psi(\underset{\sim}{\boldsymbol{\varepsilon}}^{\mathrm{e}}, \underset{\sim}{\boldsymbol{\Gamma}}) = \frac{1}{2} \underset{\sim}{\boldsymbol{\varepsilon}}^{\mathrm{e}} : \underset{\approx}{\boldsymbol{C}} : \underset{\sim}{\boldsymbol{\varepsilon}}^{\mathrm{e}} + A \frac{\Gamma}{\Gamma_0} \left(\log \frac{\Gamma_0 + \Gamma}{\Gamma_0} - 1\right), \tag{67}$$

in order to avoid the singularity of the derivative at $x_1 = 0$. This potential equation (67) is regular and convex and can be used for $\Gamma \geqslant 0$. A similar regularization was proposed in Ref. [24] for the individual logarithmic contributions of the GND densities associated with each slip system. Note that the linearization of Eq. (67) with respect to Γ leads to the quadratic potential (32). This regularization does not lead to an analytical solution.

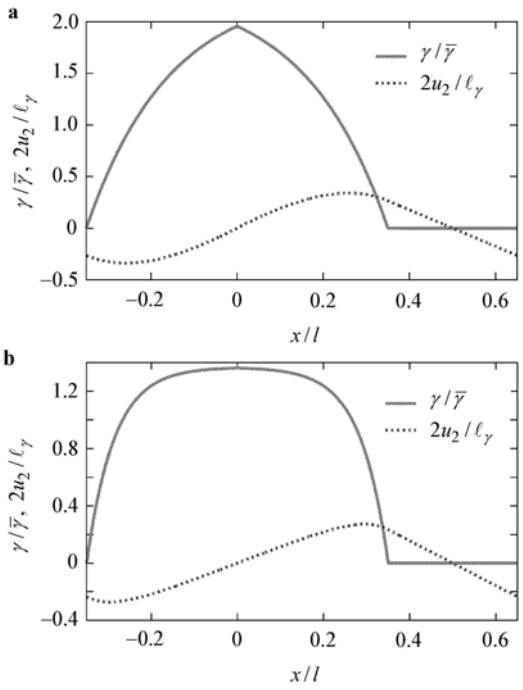

Fig. 4 Profiles of the normalized slip and displacement in the laminate for a stress value **a** $\sigma_{12} = 35\,\text{MPa}$ and **b** $\sigma_{12} = 65\,\text{MPa}$ (logarithmic potential)

5 Read–Shockley free energy potential

The potential equation (52) motivated by the statistical theory of dislocations is reminiscent of the well-known expression of the Read–Shockley energy for low angle grain boundaries [40–42]

$$\psi(\underset{\sim}{\boldsymbol{\varepsilon}}^{\mathrm{e}}, \underset{\sim}{\boldsymbol{\Gamma}}) = \frac{1}{2}\underset{\sim}{\boldsymbol{\varepsilon}}^{\mathrm{e}} : \underset{\approx}{\boldsymbol{C}} : \underset{\sim}{\boldsymbol{\varepsilon}}^{\mathrm{e}} + A\frac{\|\underset{\sim}{\boldsymbol{\Gamma}}\|}{\Gamma_0}\Big(1 - \log\frac{\|\underset{\sim}{\boldsymbol{\Gamma}}\|}{\Gamma_0}\Big), \tag{68}$$

where A and Γ_0 are material parameters. This choice amounts to considering that the energy density associated with the dislocation density tensor is estimated as that of a continuous distribution of low angle grain boundaries. It is related to the link between the dislocation density tensor and lattice curvature, embodied by Nye's well-known relation [1, 7]. Lattice curvature represents the continuum distribution of lattice misorientation which is the classical argument of Read–Shockley energy function. Note that the physical meaning of the constant Γ_0 is different from that in the expression (52). Here it is regarded as the maximum reachable value of Γ instead of the initial one. The energy density function (68) then is an increasing concave function of $0 \leqslant \Gamma \leqslant \Gamma_0$. It is continuous but not differentiable at $\Gamma = 0$.

There are therefore two reasons for considering the Read–Shockley as a candidate potential in our analysis. First, it is interesting to notice that the potential (68) is the opposite of Eq. (52) and that its physical meaning requires a different interpretation of the parameter Γ_0. Second, such dislocation walls can form inside grains in the form of kink bands resulting from strain localization, as shown in Ref. [43]. They are the precursors of grain fragmentation and subgrain formation after large deformations.

The state laws of the model are

$$\underset{\sim}{\boldsymbol{\sigma}} = \underset{\approx}{\boldsymbol{C}} : \underset{\sim}{\boldsymbol{\varepsilon}}^{\mathrm{e}}, \quad \underset{\sim}{\boldsymbol{M}} = -\frac{A}{\Gamma_0}\log\Big(\frac{\Gamma}{\Gamma_0}\Big)\frac{\underset{\sim}{\boldsymbol{\Gamma}}}{\Gamma}. \tag{69}$$

Typically the parameter Γ_0 can be estimated as the ratio $\theta_0/\ell_{\mathrm{GB}}$ where θ_0 is the maximal misorientation of low angle grain boundary and ℓ_{GB} is a typical thickness of the considered grain boundary. Taking $\theta_0 = 15^\circ$ and $\ell_{\mathrm{GB}} = 1\,\text{nm}$, we get $\Gamma_0 = 2.6 \times 10^8\,\text{m}^{-1}$. The corresponding maximum dislocation density then has the order of magnitude $\rho_{G0} = \Gamma_0/b = 5 \times 10^{16}\,\text{m}^{-2}$. The ratio A/Γ_0 has the order of magnitude E_{m}/θ_0 where E_{m} is the maximum grain boundary energy. Taking $E_{\mathrm{m}} = 1\,\text{J}\cdot\text{m}^{-2}$ gives $A/\Gamma_0 \sim 4\,\text{Pa}\cdot\text{m}$.

5.1 Solution of the two-phase laminate problem

For the two-phase laminate, the double stress tensor according to Eq. (69) takes the value

$$\begin{aligned}\underset{\sim}{\boldsymbol{M}} &= \frac{A}{\Gamma_0}\log\Big(\frac{|\gamma_{,1}|}{\Gamma_0}\Big)\frac{\gamma_{,1}}{|\gamma_{,1}|}\underline{\boldsymbol{e}}_1 \otimes \underline{\boldsymbol{e}}_3 \\ &= \frac{A}{\Gamma_0}\epsilon\log\frac{|\gamma_{,1}|}{\Gamma_0}\underline{\boldsymbol{e}}_1 \otimes \underline{\boldsymbol{e}}_3,\end{aligned} \tag{70}$$

$$\operatorname{curl}\underset{\sim}{\boldsymbol{M}} = \frac{A}{\Gamma_0}\frac{\gamma_{,11}}{|\gamma_{,1}|}\underline{\boldsymbol{e}}_1 \otimes \underline{\boldsymbol{e}}_2, \tag{71}$$

where $\epsilon = \operatorname{sgn}\gamma_{,1}$. The induced back stress then is

$$x = \operatorname{curl}\underset{\sim}{\boldsymbol{M}} : \underline{\boldsymbol{e}}_1 \otimes \underline{\boldsymbol{e}}_2 = \frac{A}{\Gamma_0}\frac{\gamma_{,11}}{|\gamma_{,1}|}. \tag{72}$$

The Schmid law requires that

$$\sigma_{12} = \tau = \tau_{\mathrm{c}} + x = \tau_{\mathrm{c}} + \frac{A}{\Gamma_0}\frac{\gamma_{,11}}{|\gamma_{,1}|}. \tag{73}$$

This is a differential equation in γ the solution of which is of the form

$$\gamma(x_1) = \alpha\Big[\exp\Big(\epsilon\frac{x_1}{L}\Big) - \exp\Big(-\frac{s}{2L}\Big)\Big], \tag{74}$$

where α is a constant to be determined and

$$\frac{1}{L} = \frac{\sigma_{12} - \tau_{\mathrm{c}}}{A}\Gamma_0. \tag{75}$$

The slip function (74) fulfills the conditions $\gamma\Big(\pm\frac{s}{2}\Big) = 0$. The shear stress can be used to compute the displacements in the soft and hard phases

$$\begin{aligned}u^s(x_1) = &\Big[\frac{\sigma_{12}}{\mu} - \overline{\gamma} - \alpha\exp\Big(-\frac{s}{2L}\Big)\Big]x_1 \\ &+\epsilon\alpha L\exp\Big(\epsilon\frac{x_1}{L}\Big) - 1.\end{aligned} \tag{76}$$

$$u^h(x_1) = \Big(\frac{\sigma_{12}}{\mu} - \overline{\gamma}\Big)x_1 + D. \tag{77}$$

The constants to be determined are α, D and σ_{12} or, equivalently, L. Two conditions are obtained from the continuity requirement of the displacement at $s/2$ and at $s/2+h$. From $u^s(s/2) = u^h(s/2)$, we get

$$D = \alpha\left[L - \exp\left(-\frac{s}{2L}\right)\left(L + \frac{s}{2}\right)\right]. \tag{78}$$

From $u^s(-s/2) = u^h(s/2+h)$, we get

$$D = \left(\bar{\gamma} - \frac{\sigma_{12}}{\mu}\right)\frac{\ell}{2}. \tag{79}$$

The two last relations have been obtained under the assumption that $\epsilon = -1$ for $x_1 \in [0 : s/2]$ and $\epsilon = 1$ for $x_1 \in [-s/2 : 0]$, which corresponds to an applied shear $\bar{\gamma} > 0$.

The slip profiles can be drawn for fixed values of the stress level, see Fig. 5. The used material parameters are those of Table 1, except that $A/\Gamma_0 = 4\,\text{kPa·mm}$. The concavity of the slip profile is opposite to that found for the previous potentials.

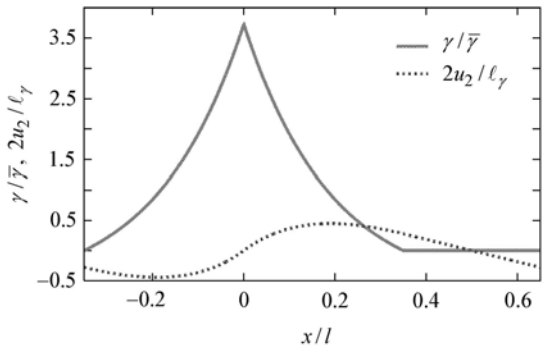

Fig. 5 Profiles of the normalized slip and displacement in the laminate for a stress value $\sigma_{12} = 22\,\text{MPa}$ (Read–Shockley potential)

6 Conclusions

Four distinct free energy functions of the dislocation density tensor have been examined in the context of strain gradient plasticity. The quadratic and rank one potentials existing in the literature have been considered first to solve the problem of the shearing of a two-phase laminate including a purely elastic phase and an elastic-plastic single crystal whose single slip plane and slip direction are perpendicular to the interface. The quadratic potential leads to a physically relevant parabolic slip profile but an unusual $1/l^2$ scaling law for the effective kinematic hardening modulus. Groma's statistical theory of dislocations has been used to motivate a new potential involving the logarithm of the norm of the dislocation density tensor, and similar to potentials proposed for individual GND densities in Refs. [22, 24]. The solution of the laminate problem leads to realistic exponential slip profiles are predicted. An alternative logarithmic potential was then proposed based on the well-known Read–Shockley low angle grain boundary energy. The corresponding slip profiles were found to have a convexity opposite to that found with Groma's potential. The size effects as predicted by the rank one and logarithmic models will be explored in a forthcoming publication [37].

The present analysis was focused on bulk free energy potentials and did not address the related question of constitutive laws for the interface or grain boundary behaviour. Continuity requirements were imposed at the interface in the laminate problem. Instead, specific interface constitutive laws can be also considered as derived by Refs. [44–51]. Interfacial gradient plasticity is also addressed in Refs. [25, 52, 53]. Additional work is needed to investigate the size effects predicted by combinations of bulk and interface models.

Jumps in the double traction were found at the interface between the elastic and elastoplastic phase. Validity of the solution then requires the external application of the corresponding double traction at the interface. Alternatively, it has been shown in Ref. [10] that the strain gradient crystal plasticity model can be regularized so that the double tractions are eventually transmitted to the elastic phase, by means of a micromorphic crystal plasticity theory. Similar extension to the micromorphic framework is possible for the free energy potentials proposed in the present paper.

Dissipative contributions associated with the increase of the dislocation density tensor have not been considered in the present work. The discussion was restricted to the free energy contribution. It is expected that both contributions are significant and that the introduction of the dissipative part is necessary in ways that are still largely open [13].

The proposed potentials and their regularized forms will be used in finite element simulations in order to work out the predicted size effect in cases where no analytical solution can be derived for laminate microstructures, but also inclusions in single crystal matrix [54] and polycrystalline aggregates [18]. For that purpose, they can be readily incorporated in the micromorphic generalizations introduced by Ref. [10] where the merits of such extensions of the strain gradient model were exhibited.

Acknowledgements The authors want to thank Dr. F. Latourte (EDF Research and Development Division, Les Renardières, Moret-sur-Loing, France) and Dr. J.M. Proix (EDF Research and Development Division, Clamart, France), and the MAI-SN (EDF, Les Renardières, Moret-sur-Loing, France) for stimulating discussions and financial support for part of this study. Fruitful discussions with Dipl.-Ing. S. Wulfinghoff are also acknowledged.

References

1 Nye, J.F.: Some geometrical relations in dislocated crystals. Acta Metall. **1**, 153–162 (1953)
2 Kröner, E.: Kontinuumstheorie der Versetzungen und Eigenspannungen. Ergebnisse der Angewandten Mathematik, 5, Springer-Verlag, Berlin (1958)
3 Cermelli, P., Gurtin, M.E.: On the characterization of geometrically necessary dislocations in finite plasticity. Journal of the

Mechanics and Physics of Solids **49**, 1539–1568 (2001)
4 Svendsen, B.: Continuum thermodynamic models for crystal plasticity including the effects of geometricallynecessary dislocations. Journal of the Mechanics and Physics of Solids **50**, 1297–1329 (2002)
5 Forest, S.: The micromorphic approach for gradient elasticity, viscoplasticity and damage. ASCE Journal of Engineering Mechanics **135**, 117–131 (2009)
6 Upadhyay, M.V., Capolungo, L., Taupin, V., et al.: Elastic constitutive laws for incompatible crystalline media: The contributions of dislocations, disclinations and G-disclinations. Philosophical Magazine **93**, 794–832 (2012)
7 Forest, S., Cailletaud, G., Sievert, R.: A Cosserat theory for elastoviscoplastic single crystals at finite deformation. Archives of Mechanics **49**, 705–736 (1997)
8 Fleck, N.A., Hutchinson, J.W.: Strain gradient plasticity. Adv. Appl. Mech. **33**, 295–361 (1997)
9 Gurtin, M.E.:A gradient theory of single–crystal viscoplasticity that accounts for geometrically necessary dislocations. Journal of the Mechanics and Physics of Solids **50**, 5–32 (2002)
10 Cordero, N.M., Gaubert, A., Forest, S., et al.: Size effects in generalised continuum crystal plasticity for two-phase laminates. Journal of the Mechanics and Physics of Solids **58**, 1963–1994 (2010)
11 Steinmann, P.: Views on multiplicative elastoplasticity and the continuum theory of dislocations. International Journal of Engineering Science **34**, 1717–1735 (1996)
12 Forest, S.: Some links between Cosserat, strain gradient crystal plasticity and the statistical theory of dislocations. Philosophical Magazine **88**, 3549–3563 (2008)
13 Gurtin, M.E., Anand, L.: Thermodynamics applied to gradient theories involving the accumulated plastic strain: The theories of Aifantis and Fleck & Hutchinson and their generalization. Journal of the Mechanics and Physics of Solids **57**, 405–421 (2009)
14 Neff, P., Sydow, A., Wieners, C.: Numerical approximation of incremental infinitesimal gradient plasticity. International Journal for Numerical Methods in Engineering **77**, 414–436 (2009)
15 Aslan, O., Cordero, N.M., Gaubert, A., et al.: Micromorphic approach to single crystal plasticity and damage. International Journal of Engineering Science **49**, 1311–1325 (2011)
16 Reddy, B.D., Wieners, C., Wolmuth, B.: Finite element analysis and algorithms for single crystal strain-gradient plasticity. International Journal for Numerical Methods in Engineering **90**, 784–804 (2012)
17 Cordero, N.M., Forest, S., Busso, E.P., et al.: Grain size effects on plastic strain and dislocation density tensor fields in metal polycrystals. Computational Materials Science **52**, 7–13 (2012)
18 Cordero, N.M., Forest, S., Busso, E.P.: Generalised continuum modelling of grain size effects in polycrystals. Comptes Rendus Mécanique **340**, 261–274 (2012)
19 Wulfinghoff, S., Böhlke, T.: Equivalent plastic strain gradient enhancement of single crystal plasticity: Theory and numerics. Proceedings of the Royal Society A **468**, 2682–2703 (2012)
20 Conti, S., Ortiz, M.: Dislocation microstructures and the effective behavior of single crystals. Arch. Rational Mech. Anal. **176**, 103–147 (2005)
21 Okumura, D., Higashi, Y., Sumida, K., et al.: A homogenization theory of strain gradient single crystal plasticity and its finite element discretization. International Journal of Plasticity **23**, 1148–1166 (2007)
22 Groma, I., Györgyi, G., Kocsis, B.: Dynamics of coarse grain grained dislocation densities from an effective free energy. Philosophical Magazine **87**, 1185–1199 (2007)
23 Berdichevsky, V.L.: Continuum theory of dislocations revisited. Continuum Mechanics and Thermodynamics **18**, 195–222 (2006)
24 Svendsen, B., Bargmann, S.: On the continuum thermodynamic rate variational formulation of models for extended crystal plasticity at large deformation. Journal of the Mechanics and Physics of Solids **58**, 1253–1271 (2010)
25 Abu Al-Rub, R.K.: Interfacial gradient plasticity governs scale–dependent yield strength and strain hardening rates in micro/nano structured metals. International Journal of Plasticity **24**, 1277–1306 (2008)
26 Kröner, E.: Dislocations in crystals and in continua: A confrontation. International Journal of Engineering Science **33**, 2127–2135 (1995)
27 Kröner, E.: Benefits and shortcomings of the continuous theory of dislocations. International Journal of Solids and Structures **38**, 1115–1134 (2001)
28 Maugin, G.A.: Thermomechanics of Plasticity and Fracture. Cambridge University Press, Cambridge (1992)
29 Forest, S., Sedláček, R.: Plastic slip distribution in two-phase laminate microstructures, Dislocation-based vs. generalized-continuum approaches. Philosophical Magazine A **83**, 245–276 (2003)
30 Kröner, E.: On the physical reality of torque stresses in continuum mechanics. Int. J. Engng. Sci. **1**, 261–278 (1963)
31 Aifantis, E.C.: The physics of plastic deformation. International Journal of Plasticity **3**, 211–248 (1987)
32 Forest, S., Aifantis, E.C.: Some links between recent gradient thermo-elasto-plasticity theories and the thermomechanics of generalized continua. International Journal of Solids and Structures **47**, 3367–3376 (2010)
33 Forest, S.: Questioning size effects as predicted by strain gradient plasticity. Journal of the Mechanical Behavior of Materials **22**, 101–110 (2013)
34 Ashby, M.F.: The deformation of plastically non-homogeneous materials. Philosophical Magazine **21**, 399–424 (1970)
35 Ohno, N., Okumura, D.: Higher-order stress and grain size effects due to self-energy of geometrically necessary dislocations. Journal of the Mechanics and Physics of Solids **55**, 1879–1898 (2007)
36 Neff, P., Sydow, A., Wieners, C.: Numerical approximation of incremental infinitesimal gradient plasticity. Int. J. for Numerical Methods in Engineering **77**, 414–436 (2009)
37 Wulfinghoff, S., Forest, S., Böhlke, T.: Logarithmic and rank-one defect energies in gradient crystal plasticity analytical and numerical 1D solutions. submitted (2013)
38 Groma, I., Csikor, F.F., Zaiser, M.: Spatial correlations and higher-order gradient terms in a continuum description of dislocation dynamics. Acta Materialia **51**, 1271–1281 (2003)
39 Yefimov, S., Groma, I., Van der Giessen, E.: A comparison of a statistical-mechanics based plasticity model with discrete dislocation plasticity calculations. J. Mech. Phys. Solids **52**, 279–300 (2004)
40 Read, W.T.: Dislocations in Crystals. McGraw-Hill, New York (1953)

41 Humphreys, F.J., Hatherly, M.: Recrystallization and Related Annealing Phenomena. Elsevier, Amserdam (2004)
42 Abrivard, G., Busso, E.P., Forest, S., et al.: Phase field modelling of grain boundary motion driven by curvature and stored energy gradients. Part I: Theory and numerical implementation. Philosophical Magazine **92**, 3618–3642 (2012)
43 Sedláček, R., Blum, W., Kratochvil, J., et al.: Subgrain formation during deformation: Physical origin and consequences. Metallurgical and Materials Transactions **33A**, 319–327 (2002)
44 Aifantis, K.E., Willis, J.R.: The role of interfaces in enhancing the yield strength of composites and polycrystals. Journal of the Mechanics and Physics of Solids **53**, 1047–1070 (2005)
45 Gurtin, M.E. Needleman, A.: Boundary conditions in small-deformation, single-crystal plasticity that account for the burgers vector. Journal of the Mechanics and Physics of Solids **53**, 1–31 (2005)
46 Acharya, A.: Jump condition for GND evolution as a constraint on slip transmission at grain boundaries. Philosophical Magazine **87**, 1349–1359 (2007)
47 Gurtin, M.E., Anand, L.: Nanocrystalline grain boundaries that slip and separate: A gradient theory that accounts for grain-boundary stress and conditions at a triple-junction. Journal of the Mechanics and Physics of Solids **56**, 184–199 (2008)
48 Fressengeas, C., Taupin, V., Upadhyay, M., et al.: Tangential continuity of elastic/plastic curvature and strain at interfaces. International Journal of Solids and Structures **49**, 2660–2667 (2012)
49 Taupin, V., Capolungo, L., Fressengeas, C., et al.: Grain boundary modeling using an elastoplastic theory of dislocation and disclination. Journal of the Mechanics and Physics of Solids **61**, 370–384 (2013)
50 Richeton, T., Berbenni, S.: Effect of heterogeneous elasticity coupled to plasticity on stresses and lattice rotation in bicrystals: A field dislocation mechanics viewpoint. European Journal of Mechanics A/Solids **37**, 231–247 (2013)
51 Berbenni, S., Paliwal, B., Cherkaoui, M.: A micromechanics-based model for shear-coupled grain boundary migration in bicrystals. International Journal of Plasticity **44**, 68–94 (2013)
52 Voyiadjis, G.Z., Faghihi, D.: Thermo-mechanical strain gradient plasticity with energetic and dissipative length scales. International Journal of Plasticity **30–31**, 218–247 (2012)
53 Voyiadjis, G.Z., Faghihi, D.: Gradient plasticity for thermo-mechanical processes in metals with length and time scales. Philosophical Magazine **93**, 1013–1053 (2013)
54 Chang, H.J., Gaubert, A., Fivel, M., et al.: Analysis of particle induced dislocation structures using three-dimensional dislocation dynamics and strain gradient plasticity. Computational Materials Science **52**, 33–39 (2012)